TUM-HEP-395/00

December 2000

# Chargino searches at LEP for complex MSSM parameters[1]

Nabil Ghodbane[a], Stavros Katsanevas[a], Imad Laktineh[a] and Janusz Rosiek[b,2]

[a] *Institut de Physique Nucléaire de Lyon*
*43 Bd du 11 novembre 1918, 69622 Villeurbanne cedex, France*

[b] *Physik Department, Technische Universität München*
*D-85748 Garching, Germany*

## Abstract

We reanalyze the results of the chargino searches at LEP (on the basis of the DELPHI 189 GeV data sample), including the possibility of complex MSSM parameters. We point out the possible differences between the complex- and real-parameter analysis. We check that the regions excluded by "standard" analyses remain generally robust against the introduction of complex parameters, with the exception of light sneutrino and low $\tan\beta$ scenario, where additional constraints like those given by the $Z^0$ width or electric dipole moment measurements are necessary.

[1] This work was supported in part by the Polish Committee for Scientific Research under the grant number 2 P03B 052 16 and by the French-Polish exchange program POLONIUM project 01391TB.

[2] On leave of absence from Institute of Theoretical Physics, Warsaw University, Hoża 69, 00-681 Warsaw, Poland

# 1 Introduction

In the Minimal Supersymmetric Standard Model (MSSM) there are new potential sources of CP non-conservation effects. One can distinguish two categories of such sources. One is independent of the physics of flavor non-conservation in the neutral current sector and the other is closely related to it. The first category is particularly interesting from the point of view of collider experiments as it may affect the direct searches for the supersymmetric Higgs bosons [1] and other particles. Complex phases may be present several flavor-conserving parameters of the MSSM Lagrangian: $\mu$ parameter, gaugino masses $M_i$, trilinear scalar couplings $A_i$ and soft Higgs mixing term $m_{12}^2$. In principle they can be arbitrary (although not all of them are physically independent).

Experimental constraints on the "flavor-conserving" phases come mainly from the electric dipole moments of electron [2] and neutron [3]:

$$E_e^{exp} < 4.3 \cdot 10^{-27} e \cdot cm$$
$$E_n^{exp} < 6.3 \cdot 10^{-26} e \cdot cm$$

Until recently, the common belief was that the constraints from the electron and neutron electric dipole moments are strong [4] and the new phases must be very small. More recent calculations performed in the framework of the minimal supergravity model [5, 6, 7] and non-minimal models [8] indicated the possibility of cancellations between contributions proportional to the phase of $\mu$ and those proportional to the phase of $A$ and, therefore, of weaker limits on the phases in a non-negligible range of parameter space. The detailed analysis [9] showed that the constraints on the phases (particularly on the phase of $\mu$ and of the gaugino masses) are generically strong ($\phi \leq 10^{-2}$) if all relevant supersymmetric masses are light, say below $\mathcal{O}(300$ GeV). However, the constraints disappear or are substantially relaxed if just some of those masses, e.g. slepton and sneutrino masses, are large, $m_E > \mathcal{O}(1$ TeV). Thus, the phases can be large even if some masses, e.g. the chargino masses, are small. In the parameter range where the constraints are generically strong, there exist fine-tuned regions where cancellations between different contributions to the EDM can occur even for large phases. They require not only $\mu - A$, $\mu - M_{gaugino}$ or $M_1 - M_2$ phase adjustments but also values of soft mass parameters strongly correlated with the phases and among themselves (especially for higher values of $\tan\beta$, as the constraints on $\mu$ phase scale as $1/\tan\beta$). Nevertheless, since the notion of fine tuning is not precise, particularly from the point of view of GUT models, it is not totally inconceivable that the rationale for large cancellations exists in the large energy scale physics [10]. Therefore all experimental bounds on the supersymmetric parameters should include the possibility of substantial phases allowing the possibility of large cancellations, to claim full model independence.

We define the new flavor-conserving phases in the MSSM as:

$$e^{i\phi_\mu} = \frac{\mu}{|\mu|} \qquad e^{i\phi_i} = \frac{M_i}{|M_i|} \qquad e^{i\phi_{A_I}} = \frac{A_I}{|A_I|} \qquad e^{i\phi_H} = \frac{m_{12}^2}{|m_{12}^2|} \tag{1}$$

Not all of those phases are physical (see [9] for a more detailed discussion). Physics observables depend only on the phases of some parameter combinations. Such combinations are:

$$M_i\mu(m_{12}^2)^\star \qquad A_I\mu(m_{12}^2)^\star \qquad A_I^\star M_i \tag{2}$$

Not all of them are independent: two of the phases can be rotated away. We follow the common choice and keep $m_{12}^2$ real in order to have real tree level Higgs field VEV's and $\tan\beta$[3]. The second re-phasing may be used e.g. to make one of the gaugino mass terms real - we choose it to be $M_2$. With this choice, chargino production cross section is sensitive only to the $\mu$ parameter phase. Neutralino production and chargino/neutralino decay rates may depend additionally on the $M_1$ phase, but for the purpose of this analysis we assume universal gaugino masses at the GUT scale. In such a case low-energy values of $M_1$ and $M_2$ are connected by the relation $M_1 = 5/3\tan^2\theta_W M_2$ and the identical phases of $M_1$ and $M_2$ can be simultaneously rotated away. In section 5 we discuss the possible effects of the departure from this assumption.

This paper is organized as follows. In section 2 we present the general expressions for chargino and neutralino production cross section for the case of complex couplings. In section 3 we define the range of scan over the MSSM parameters we use and we discuss the possible effects of phases on chargino masses, production and decay rates. In section 4 we present the results of our scan, comparing the expected chargino production and decay rates to the experimental results obtained by DELPHI. Several points where the introduction of complex parameters could endanger the model-independence of the experimental limits are found. Then, in section 5, we examine ways to restore the real-parameter exclusion limits by the use of the EDM measurements as an additional constraint. We finally present our conclusions in section 6. The necessary conventions and Feynman rules are collected in the Appendix.

# 2 Cross sections for the chargino and neutralino production

In this sections we list the formulae for the chargino and neutralino production cross section in $e^+e^-$ collisions for the general case of complex couplings. For completeness, here and in

[3]Loop corrections to the effective potential induce phases in VEV's even if they were absent at the tree level. Rotating them away reintroduces a phase into the $m_{12}^2$ parameter.

the Appendix we give the most general expressions, including also the possibility of flavor mixing of sneutrinos (we neglect only the very small right-handed couplings of charginos to electrons, $S_{RC} \sim \mathcal{O}\left(\frac{em_e \tan\beta}{M_W}\right)$). However, in our numerical analysis we consider only the simplified case, neglecting possible inter-generational sneutrino mixing.

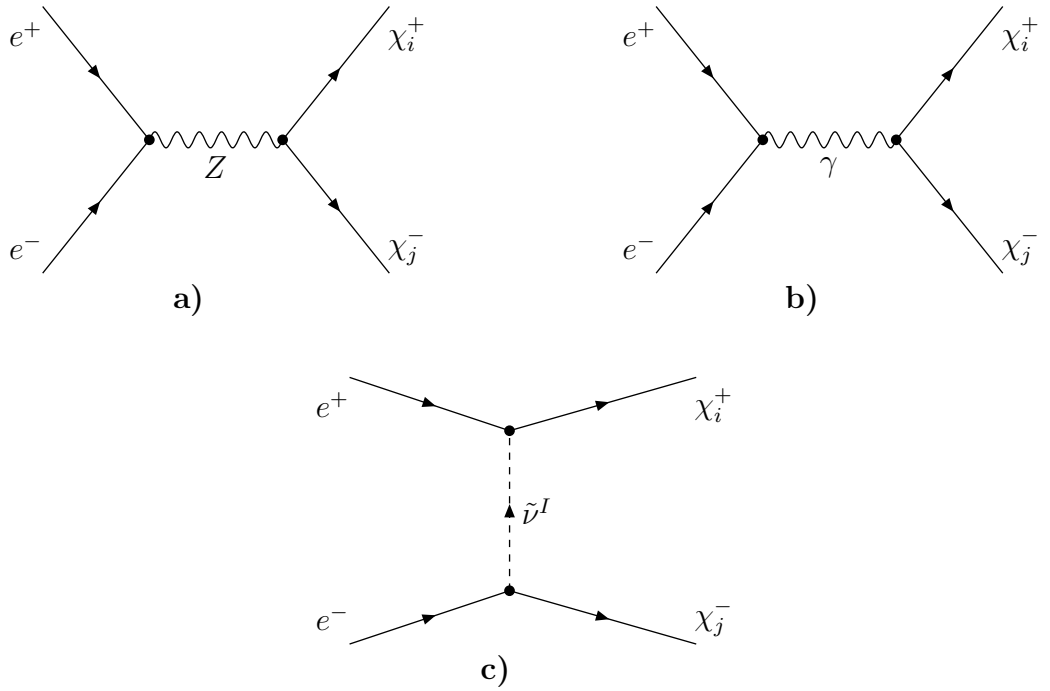


Figure 1: Diagrams contributing to chargino production in $e^+e^-$ collisions.

The chargino production amplitude is given by the three diagrams shown in fig. 1. Using the notation defined in Appendix, the differential cross section in the CMS frame for the process $e^+e^- \to \chi_i^+\chi_j^-$ can be written as:

$$\frac{d\sigma(e^+e^- \to \chi_i^+\chi_j^-)}{d\Omega} = \frac{\lambda(s, m_i^2, m_j^2)}{64\pi^2 s^2}\left(M_{aa} + M_{bb} + M_{cc} + M_{ab} + M_{ac} + M_{bc}\right) \tag{3}$$

where $m_i \equiv m_{\chi_i^+}$, $m_j \equiv m_{\chi_j^+}$, $\lambda(x,y,z) = (x^2+y^2+z^2-2xy-2xz-2yz)^{1/2}$ and $M_{xy}$ respond to contributions of respective diagrams in fig. 1 and their interference:

$$\begin{aligned} M_{aa} &= \frac{e^2}{4|D_Z(s)|^2}\Big[(a_e^2+b_e^2)\left((|V_{LC}^{ij}|^2+|V_{RC}^{ij}|^2)\left(s^2-(m_i^2-m_j^2)^2+\lambda^2\cos^2\theta\right)\right. \\ &+ \left. 8sm_im_j\mathrm{Re}(V_{LC}^{ij}V_{RC}^{ij\star})\right) - 2(a_e^2-b_e^2)(|V_{LC}^{ij}|^2-|V_{RC}^{ij}|^2)s\lambda\cos\theta\Big] \qquad (4) \\ M_{bb} &= \frac{e^4}{s^2}\left(s^2+4sm_i^2+\lambda^2\cos^2\theta\right)\delta_{ij} \qquad (5) \\ M_{cc} &= \frac{e^4}{16s_W^4|D_{\tilde{\nu}}(t)|^2}|Z_+^{1i}Z_+^{1j}|^2\left[(s-\lambda\cos\theta)^2-(m_i^2-m_j^2)^2\right] \qquad (6) \end{aligned}$$

$$
\begin{aligned}
M_{ab} &= \frac{e^3(s-M_Z^2)}{2s|D_Z(s)|^2}\Big((a_e+b_e)(V_{LC}^{ii}+V_{RC}^{ii})\left(s^2+4sm_i^2+\lambda^2\cos^2\theta\right) \\
&- 2(a_e-b_e)(V_{LC}^{ii}-V_{RC}^{ii})s\lambda\cos\theta\Big)\,\delta_{ij} \qquad (7)\\
M_{ac} &= \frac{e^3 a_e}{4s_W^2}\mathrm{Re}\left(\frac{V_{LC}^{ij}\left((s-\lambda\cos\theta)^2-(m_i^2-m_j^2)^2\right)+4V_{RC}^{ij}sm_im_j}{D_Z^\star(s)D_{\tilde\nu}(t)}Z_+^{1i}Z_+^{1j\star}\right) \qquad (8)\\
M_{bc} &= \frac{e^4}{4s_W^2 sD_{\tilde\nu}(t)}|Z_+^{1i}|^2\left((s-\lambda\cos\theta)^2+4sm_i^2\right)\delta_{ij} \qquad (9)
\end{aligned}
$$

By $a_e, b_e$ we denoted the left and right part of the $Z\bar{e}e$ coupling, $ie(a_eP_L+b_eP_R)$ (so that $a_e=(2s_W^2-1)/2s_Wc_W$, $b_e=s_W/c_W$), $D_Z(s)=s-M_Z^2+iM_Z\Gamma_Z$, $t=\frac{1}{2}(m_i^2+m_j^2-s+\lambda\cos\theta)$ and $D_{\tilde\nu}(t)$ is "flavor averaged" $t$-channel sneutrino propagator (for vanishing sneutrino mixing it reduces simply to electron sneutrino propagator):

$$
\frac{1}{D_{\tilde\nu}(t)}=\sum_{I=1}^{3}\frac{|Z_{\tilde\nu}^{1I}|^2}{t-m_{\tilde\nu^I}^2} \qquad (10)
$$

The total cross section for the chargino pair production reads as:

$$
\sigma(e^+e^-\to\chi_i^+\chi_j^-)=\frac{\lambda(s,m_i^2,m_j^2)}{16\pi s^2}\left(\mathcal{M}_{aa}+\mathcal{M}_{bb}+\mathcal{M}_{cc}+\mathcal{M}_{ab}+\mathcal{M}_{ac}+\mathcal{M}_{bc}\right) \qquad (11)
$$

where $\mathcal{M}_{xy}$ are:

$$
\begin{aligned}
\mathcal{M}_{aa} &= \frac{e^2(a_e^2+b_e^2)}{4|D_Z(s)|^2}\left[(|V_{LC}^{ij}|^2+|V_{RC}^{ij}|^2)\left(s^2-(m_i^2-m_j^2)^2+\frac{\lambda^2}{3}\right)\right. \qquad (12)\\
&+ \left. 8sm_im_j\mathrm{Re}(V_{LC}^{ij}V_{RC}^{ij\star})\right] \qquad (13)\\
\mathcal{M}_{bb} &= \frac{4e^4}{3s}\left(s+2m_i^2\right)\delta_{ij} \qquad (14)\\
\mathcal{M}_{cc} &= \frac{e^4}{4s_W^4}|Z_+^{1i}Z_+^{1j}|^2\sum_{I,J=1}^{3}|Z_{\tilde\nu}^{1I}Z_{\tilde\nu}^{1J}|^2\,[1 \\
&+ \left. 2\frac{(m_{\tilde\nu^I}^2-m_i^2)(m_{\tilde\nu^I}^2-m_j^2)L(m_{\tilde\nu^I}^2)-(m_{\tilde\nu^J}^2-m_i^2)(m_{\tilde\nu^J}^2-m_j^2)L(m_{\tilde\nu^J}^2)}{\lambda(m_{\tilde\nu^I}^2-m_{\tilde\nu^J}^2)}\right] \qquad (15)\\
\mathcal{M}_{ab} &= \frac{2e^3(a_e+b_e)(s-M_Z^2)}{3|D_Z(s)|^2}(V_{LC}^{ii}+V_{RC}^{ii})(s+2m_i^2)\delta_{ij} \qquad (16)\\
\mathcal{M}_{ac} &= \frac{e^3a_e}{2s_W^2}\sum_{I=1}^{3}|Z_{\tilde\nu}^{1I}|^2\mathrm{Re}\left[\frac{Z_+^{1i}Z_+^{1j\star}}{D_Z^\star(s)}\left(V_{LC}^{ij}\left(2m_{\tilde\nu^I}^2-m_i^2-m_j^2-s\right.\right.\right. \\
&+ \left.\left.\left.\frac{2((m_{\tilde\nu^I}^2-m_i^2)(m_{\tilde\nu^I}^2-m_j^2))}{\lambda}L(m_{\tilde\nu^I}^2)\right)+V_{RC}^{ij}\frac{2sm_im_j}{\lambda}L(m_{\tilde\nu^I}^2)\right)\right] \qquad (17)\\
\mathcal{M}_{bc} &= \frac{e^4}{s_W^2 s}\delta_{ij}|Z_+^{1i}|^2\sum_{I=1}^{3}|Z_{\tilde\nu}^{1I}|^2\left[m_{\tilde\nu^I}^2-m_i^2-\frac{1}{2}s+\frac{(m_{\tilde\nu^I}^2-m_i^2)^2+sm_i^2}{\lambda}L(m_{\tilde\nu^I}^2)\right] \qquad (18)
\end{aligned}
$$

where we defined function $L$ as

$$L(m^2_{\tilde{\nu}^I}) = \log\left(\frac{2m^2_{\tilde{\nu}^I} - m_i^2 - m_j^2 + s - \lambda}{2m^2_{\tilde{\nu}^I} - m_i^2 - m_j^2 + s + \lambda}\right) \tag{19}$$

For the purpose of this paper we use only the neutralino production cross section at the $Z^0$ peak, in order to calculate the invisible $Z^0$ decay width. Thus, it is sufficient to include only the $s$-channel diagram in the expression for the neutralino production amplitude. In this approximation, the differential cross section in the CMS frame for the process $e^+e^- \to \chi_i^0\chi_j^0$ has a simple form:

$$\begin{aligned}\frac{d\sigma(e^+e^- \to \chi_i^0\chi_j^0)}{d\Omega} &= \frac{(2-\delta_{ij})e^2(a_e^2+b_e^2)\lambda(s,m_i^2,m_j^2)}{64\pi^2 s^2|D_Z(s)|^2}\Big[|V_N^{ij}|^2\left(s^2-(m_i^2-m_j^2)^2+\lambda^2\cos^2\theta\right)\\ &- 4sm_im_j\mathrm{Re}(V_N^{ij})^2\Big]\end{aligned} \tag{20}$$

where now $m_i \equiv m_{\chi_i^0}$, $m_j \equiv m_{\chi_j^0}$.

The total cross section for the process $e^+e^- \to \chi_i^0\chi_j^0$ reads as:

$$\begin{aligned}\sigma(e^+e^- \to \chi_i^0\chi_j^0) &= \frac{(2-\delta_{ij})e^2(a_e^2+b_e^2)\lambda(s,m_i^2,m_j^2)}{16\pi s^2|D_Z(s)|^2}\left[|V_N^{ij}|^2\left(s^2-(m_i^2-m_j^2)^2+\frac{\lambda^2}{3}\right)\right.\\ &- \left. 4sm_im_j\mathrm{Re}(V_N^{ij})^2\right]\end{aligned} \tag{21}$$

# 3 Features of the chargino searches for the complex MSSM parameters

In order to check the effects of introduction of complex couplings on LEP limits, we performed a scan over the parameters present in the gaugino mass matrices and the chargino couplings. These parameters are:

- $|\mu|$, modulus of the Higgs mixing parameter. We assumed it running from 5 to 500 GeV, with a step of 5 GeV.

- $M_2$, the $SU(2)$ gaugino mass. We scan over it in the same range as for the parameter $|\mu|$: 5 to 500 GeV and the same step. We also assume that the GUT relation between the gaugino masses holds: $M_1 = \frac{5}{3}\tan\theta_W^2 M_2$. In this case, the common gaugino mass parameter phase can be rotated away and both $M_1, M_2$ can be chosen to be real.

- $m_{\tilde{\nu}_e}$, the mass of the electron sneutrino, contributing to the $t$-channel diagram in the chargino production cross section. We consider the cases for which the sneutrino mass is 45, 50, 60, 70, 80, 90, 100, 110, 200 and 300 GeV.

- $\tan\beta$ parameter. We consider three values: two small ones $\tan\beta = 1, 1.5$ and one large $\tan\beta = 35$.

- Finally, we perform the scan over $\phi_\mu$, the phase of the $\mu$ parameter, from 0 to $\pi$ with a step of $\pi/18$ (variation of $\phi_\mu$ in the extended range $0 - 2\pi$ leads to identical results).

- The right selectron mass was fixed to be at high value (300 GeV). It only comes in the chargino decay to neutralino plus leptons, and might alter some of the branching fractions, but since we already scan over the sneutrino and therefore the left selectron mass, the possibility of a light charged slepton is taken into account. It is also worth noting that the assumption of heavy right selectron is a conservative one for what concerns the EDM constraints on $\mu$ phase.

The output of our scan are the physical gaugino masses, the chargino cross sections and branching ratios for a center mass energy of 189 GeV as well as the neutralino and chargino contributions to the $Z^0$ width. We computed these using the SUSYGEN 3 program [13], whose independent calculation of the chargino and neutralino production cross sections has been checked against the formulae in section 2.

### 3.1 Effects of complex parameters on physical masses

Figure 2 shows the chargino mass distributions in the $(M_2, |\mu|)$ plane for chosen values of the $\mu$ phase and a low value of $\tan\beta$. The first feature worth noting is that the chargino mass never decreases with the $\mu$ phase increasing from 0 (real positive $\mu$) to $\pi$ (real negative $\mu$) for any value of the remaining MSSM parameters. This is even more obvious from figure 4, where the chargino and neutralino mass dependence on $\phi_\mu$ is shown for selected values of the remaining MSSM parameters. Another feature that one can notice in figure 2 is the presence of the well known region of very low chargino masses for small $\phi_\mu$ values and the emergence of a high chargino mass corridor for $M_2 \sim |\mu| \tan\beta$ and increasing $\phi_\mu$.

In figure 3.1 we also plotted contour lines of the constant chargino-lightest neutralino mass splitting. One can see that for small $\phi_\mu$ there is an unphysical region where the chargino becomes lighter than the neutralino. One can also see the striking feature that for pure imaginary $\mu$ the region of chargino-neutralino degeneracy at high $M_2$ and low $|\mu|$ is greatly enhanced, endangering the efficiency of the experimental searches.

In general, one can observe the following types of relations between the chargino and neutralino masses as a function of $\phi_\mu$:

- The chargino/neutralino masses depend weakly on $\phi_\mu$ for high $\tan\beta$, since then some of the off-diagonal elements in the mass matrices are very small, depressing the effects

Figure 2: Contours of the constant chargino mass on the $(M_2, |\mu|)$ plane for $\tan\beta = 1.5$ and $\phi_\mu = 0, \pi/2, 3\pi/4, \pi$.

$$[\text{width=0.48}]\text{fx1p}_f x01 - snue = 70 - phimu = 0.eps[width = 0.48]fx1p_f x01 - snue = 70 - phimu = 90.eps[width = 0.48]fx1p_f x01 - snue = 70 - phimu = 135.eps[width = 0.48]fx1p_f x01 - snue = 70 - phimu = 180.eps$$

Figure 3: Contours of the constant chargino-lightest neutralino mass difference on the $(M_2, |\mu|)$ plane for $\tan\beta = 1.5$ and $\phi_\mu = 0, \pi/2, 3\pi/4, \pi$.

of $\mu$ phase on physical masses (left upper plot in fig. 4).

- The chargino mass shows a dependence on $\phi_\mu$ whereas the $\chi_1^0$ mass evolves very slowly. The chargino-neutralino mass difference is always positive and its largest value is obtained for real negative $\mu$ values (right upper plot in fig. 4).

- The same configuration can have the extreme case where for real positive $\mu$ ($\phi_\mu = 0$) one has chargino almost degenerate with the lightest neutralino, whereas for real negative $\mu$, one has a large mass difference and even cascade decays through $\chi_2^0$ (fig. 4, left lower plot).

- Finally, as it has been already shown in the previous two-dimensional figures, and it is a well known fact since some time, one has a region where the chargino becomes lighter than the neutralino for low $M_2$ values, real positive $\mu$ and small $\tan\beta$. In the right lower plot of fig. 4 one can see how the masses evolve with $\phi_\mu$ restoring the normal hierarchy between them.




Figure 4: Chargino and neutralino mass evolution as a function of $\phi_\mu$.

We systematically looked for areas, where the limits obtained by the LEP experimental searches, assuming real $\mu$, could be endangered by the introduction of the $\mu$ phase. We thus searched for regions of degeneracy between the chargino and lightest neutralino, located far from the two extreme phase values (0 and $\pi$, giving real positive and real negative $\mu$). Needless

to point out that degeneracies like that make the experimental detection very difficult, if not impossible, since the latter depends critically on the size of the visible mass difference. As it was shown generically in figure 3.1 and more specifically in figure 5, one can find parameter values for which neutralino and chargino masses are very closely degenerate for $\phi_\mu = \pi/2$, i.e. for pure imaginary $\mu$. Figure 5 shows that this feature is characteristic of a whole region around $|\mu| = 70$GeV, for $\tan\beta = 1$.

[width=0.6]masses6.eps

Figure 5: Example of extreme chargino/neutralino mass degeneracy for pure imaginary $\mu$.
[width=0.6]tb1-fx1p$_f x01 - snue = 70 - phimu = 90.eps$

Figure 6: Contours of the constant chargino-lightest neutralino mass difference on the $(M_2, |\mu|)$ plane for $\tan\beta = 1$ and $\phi_\mu = \pi/2$.

Such a situation occurs for $\tan\beta$ close to 1 (a value which is however already strongly disfavored by the direct SUSY Higgs particle searches) and $M_2/|\mu| \gg 1$, i.e. when the lighter chargino and the two lighter neutralinos are almost pure Higgsinos. In such a case one may estimate analytically that for real $\mu$ chargino-neutralino mass difference is:

$$m^2_{\chi_1^+} - m^2_{\chi_1^0} \approx \begin{cases} \frac{2m_Z^2 s_W^2 |\mu|}{M_1} & \phi_\mu = 0 \\ \\ \frac{2m_W^2 |\mu|}{M_2} & \phi_\mu = \pi \end{cases} \tag{22}$$

whereas for the pure imaginary $\mu$ the analogous formulae can be written down as:

$$m^2_{\chi_1^+} - m^2_{\chi_1^0} \approx \frac{|\mu|^2 m_Z^2 s_W^2}{M_1^2 - |\mu|^2} \approx \frac{2|\mu|^2 m_Z^2 s_W^2}{M_1^2} \tag{23}$$

The mass difference for the $\phi_\mu = \pi/2$ is suppressed by one more power of the $|\mu|/M_1$ ratio than for the real $\mu$, thus decreases much faster for fixed $|\mu|$ and heavy gauginos.

## 3.2 Effects of complex parameters on cross sections and branching fractions

Figure 7 shows the cross-section distributions in the $(M_2, |\mu|)$ plane for chosen values of the phase and a low value of $\tan\beta$ and sneutrino mass of 70 GeV.

As expected [14] the chargino production cross section depends on $\phi_\mu$ in most cases through the kinematical effects, i.e. through the chargino mass dependence on $\phi_\mu$. One can for instance see in the left plot of fig. 8 a strong phase space dependence of the cross section, as the chargino mass increases from below to above the kinematical threshold. Nevertheless, the

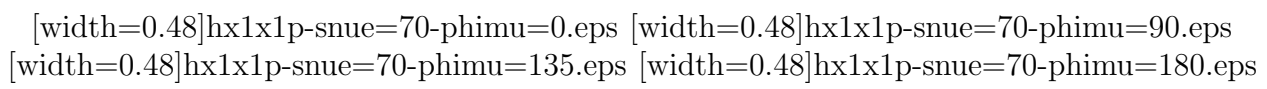

Figure 7: Contours of the constant chargino production cross section on the $(M_2, |\mu|)$ plane for $\tan\beta = 1.5$, sneutrino mass 70 GeV and $\phi_\mu = 0, \pi/2, 3\pi/4, \pi$.

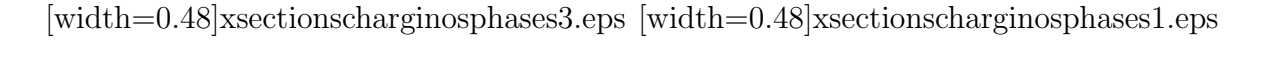

Figure 8: Cross section for the chargino production as a function of $\phi_\mu$ for two chosen sets of MSSM parameters and several sneutrino masses (marked close to the corresponding curves).

couplings involving the sneutrino also depend on $\mu$ phase, and therefore one could observe some important non-kinematical dependencies.

A particularly interesting, from the point of view of this paper, is the case where the minimal cross section does not occur for one of the two real $\mu$ values, examined by LEP, but it is reached for some $\mu$ phase between 0 and $\pi$. This is illustrated with the right plot of figure 8. One can see that for higher values of the sneutrino mass, e.g. greater than 100 GeV, the minimal cross section is obtained, as could be expected, for real negative $\mu$. But once one considers small sneutrino masses, this does not hold anymore and one finds minimal cross section for complex $\mu$. It can be a potential loophole for the LEP limits.

The branching ratios do not show any dramatic effects. For high $\tan\beta$ and for low $\tan\beta$ and high sneutrino masses they are very weakly dependent on the $\mu$ phase. For low $\tan\beta$ and low sneutrino masses the branching ratios dependence on $\phi_\mu$ can be explained by the increase of the chargino mass at large $\phi_\mu$ and therefore the opening of the direct decay channel to sneutrinos. This fact is a transcription in the complex parameter language of the well known fact that for negative $\mu$ one has enhanced leptonic branching fractions. This is illustrated in figure 9, where the leptonic branching ratio is shown as a function of $\phi_\mu$, in parallel with the chargino/neutralino mass dependence.

It is a general observation that the branching ratios do not have any local minima between $\phi_\mu = 0$ and $\pi$ and therefore we can neglect for the time being the different experimental sensitivities to different chargino pair production signatures (fully leptonic, fully hadronic and "semileptonic" decays). It is still possible that a detailed comparison of expectations and data for each signature finds weak points, where more luminosity is needed to actually exclude them for a given complex phase. But we hope the arguments above are sufficient to indicate that there is no fundamental problem that an increase of statistics (the LEP experiments currently have collected more than 10 times the statistics used in this analysis) cannot cure. We therefore choose to ignore the detailed development of the individual signatures for this

Figure 9: Branching ratios for leptonic chargino decays as a function of $\phi_\mu$, for $\tan\beta = 1.5$, $M_2 = 60$ GeV, $|\mu| = 140$ GeV and several values of the sneutrino mass.

study.

# 4 LEP limits revisited

We saw in the previous subsections three ways by which the introduction of $\mu$ phase could affect the LEP limits, obtained under the assumption of real MSSM parameters. The presence of non-trivial $\mu$ phase can introduce extra degeneracies between the chargino and neutralino physical masses or/and new cross section minima for complex $\mu$. We thus will examine, for each MSSM point, whether the introduction of a new phase either increases the chargino/neutralino degeneracy or suppresses the cross section.

In this section we revisit the exclusions given by the DELPHI collaboration with the 189 GeV data [15] for a total integrated luminosity of 158 pb$^{-1}$ collected at this energy. In the experimental analysis six mass windows have been considered (see Table 1) for 76 MSSM analysis points[4]. This experimental analysis is not sensitive to mass differences between the chargino and the neutralino below 3 GeV. We therefore consider the points with a mass degeneracy below 3 GeV, for either real or complex $\mu$, as not excluded. There exist LEP analyses [19], addressing this problem, and studying the chargino production down to very low mass differences, but their inclusion is beyond the scope of this paper.

| | $M_{\chi_1^+} - M_{\chi_1^0}$ regions |
|---|---|
| 1 | $3 \leq M_{\chi_1^+} - M_{\chi_1^0} <$ 5 GeV |
| 2 | $5 \leq M_{\chi_1^+} - M_{\chi_1^0} < 10$ GeV |
| 3 | $10 \leq M_{\chi_1^+} - M_{\chi_1^0} < 25$ GeV |
| 4 | $25 \leq M_{\chi_1^+} - M_{\chi_1^0} < 35$ GeV |
| 5 | $35 \leq M_{\chi_1^+} - M_{\chi_1^0} < 50$ GeV |
| 6 | $50 \leq M_{\chi_1^+} - M_{\chi_1^0}$ |

Table 1: Mass windows used in the interpretation of chargino searches based on the $\sqrt{s} = 189$ GeV DELPHI data [15].

We first scanned the MSSM parameters, listed in the beginning of this section, assuming

[4]We wish to thank here T. Alderweireld for providing us with the experimental data for each point used in the DELPHI paper.

$\mu$ to be real. We compared the theoretical predictions for the cross-sections with the experimental sensitivity. Figure 10 shows the excluded range in the $(M_2, \mu)$ plane, consistent with

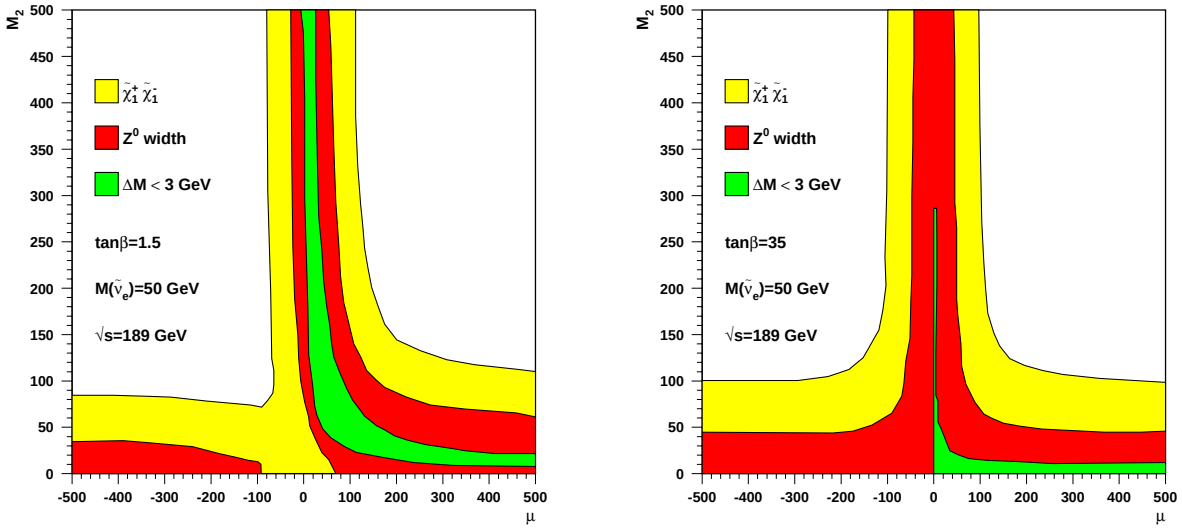


Figure 10: Excluded areas on the ($M_2$,$\mu$) plane for the sneutrino mass 50 GeV (assuming $\mu$ to be real).

the one published in [15]. The inclusion of $\mu$ phase, makes this "standard" way of presenting the excluded area obsolete. One does not have anymore two possible values for the phase of $\mu$ (0 and $\pi$), but a continuous spectrum. We need therefore to present the exclusions in the $(M_2, |\mu|)$ plane. The excluded range of figure 10, obtained under the assumption of the reality of $\mu$, has to be "folded" around the $M_2$ axis, so that the new region consists of only the points excluded, at a given $M_2$, for *both* $\phi_\mu = 0$ and $\phi_\mu = \pi$, i.e. is given by the common part of regions excluded for the two extreme $\mu$ phase values. Actually, it essentially coincides with the excluded range obtained for real negative $\mu$, "reflected" around the $M_2$ axis. We also report on the same figure, with a different (dark grey) color, the regions where the point is excluded for only one, negative or positive, value of $\mu$.

We then check, scanning over the phase of $\mu$, with a step $\pi/18$, whether the excluded area obtained in this way remains valid for any $\phi_\mu$. Simultaneously we scan also over the different values of sneutrino mass and over $\tan\beta$.

As is also custom in "real-parameter" analyses, we add the constraints coming from the $Z^0$ decay width into unknown particles. This is of great help, mostly for regions of high degeneracy. The experimental limit used, is [16]:

$$\Gamma_{new} \leq 6.4\text{MeV at } 95\% \text{ C.L.} \tag{24}$$

The value (24) can be translated into an upper limit on the total cross section associated with the production of new particles (in our case charginos and neutralinos) at $\sqrt{s} = M_Z$. The maximal allowed cross section for supersymmetric particle production is $\sigma_{new} \leq 152$ pb at 95% C.L. The contributions are of course calculated with the formulae derived for the complex MSSM parameters.

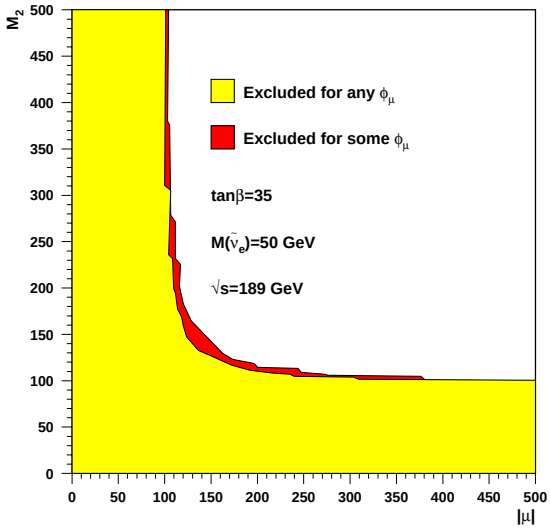


Figure 11: Excluded areas in the $(M_2, |\mu|)$ plane for large $\tan\beta$.

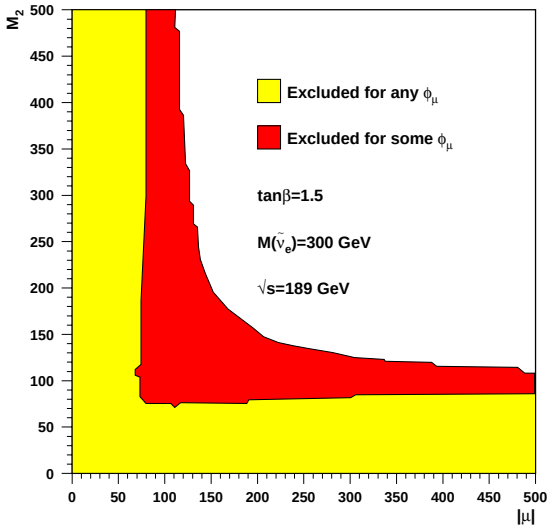


Figure 12: Excluded areas in the $(M_2, |\mu|)$ plane for small $\tan\beta$ and heavy sneutrino.

For large $\tan\beta$, the excluded region remains robust, and fully connected, for any sneutrino masses. This result is illustrated with figure 11. The same is true for small values of $\tan\beta$ and high sneutrino masses, as can be seen in figure 12.

The situation is more complicated for small values of $\tan\beta$ and low sneutrino masses. For low sneutrino masses, in the range 50-80 GeV, one finds large areas not excluded anymore inside the region that is normally excluded for real value $\mu$'s. This is illustrated by figure 4. One can remark that for these areas $M_2$ and $|\mu|$ are connected by the approximate relation $M_2 \sim \mu \tan\beta$. It is the well known low sensitivity region, problematic even for real parameter analyses, and concerns the $\mu$ phases close to $\pi$. The landscape becomes a little more complicated for $\tan\beta$ exactly equal to 1, where as was shown in the previous section, there is a new high degeneracy region developing around $|\mu| = 70$ GeV. Figure 4, shows these two types (low cross section and high degeneracy) of not-excluded regions for $\tan\beta = 1$ and sneutrino mass of 45 GeV. Here, we have to stress once more, that the Higgs searches, analyzed under the

assumption of complex phases [18], have most probably excluded the value of $\tan\beta = 1$. The analysis of [18] having an indicative character, when repeated by the LEP working groups, could firmly establish the complementary role of Higgs to chargino searches in what regards phases.

[width=0.48]exclusion1.5$_5$0$_2$.*eps*[*width* = 0.48]*exclusion*1.5$_7$0$_2$.*eps*

Figure 13: Excluded areas in the $(M_2, |\mu|)$ plane for small $\tan\beta$ and light sneutrino.

[width=0.48]exclusion1$_4$5$_2$.*eps*

Figure 14: Excluded areas in the $(M_2, |\mu|)$ plane for $\tan\beta = 1$ and light sneutrino.

Hence, as a first conclusion, we can say that, taking into account the non-trivial phase of the $\mu$ parameter in the chargino searches at LEP may lead to the appearance (or the enlarging, compared to the standard analysis) of unexcluded areas in the $(M_2, |\mu|)$ plane. These are:

a) A pronounced unexcluded region for light sneutrino $m_{\tilde{\nu}} \sim 50 - 70$ GeV and small value of $\tan\beta$. This is due to local minima of the cross sections, and can be cured by a simple increase in statistics. Indeed the real-parameter exclusions can be restored if we arbitrarily scale by a factor 9 the statistics of the data-sample used. The present data-sample by all 4 LEP experiments, corresponds certainly to more than 10 times the luminosity than the one used here.

b) An unexcluded region around $\phi = \pi/2$, for purely imaginary $\mu$, and $\tan\beta = 1$ which is due to an increase of the degeneracy region, and the subsequent lowering of the experimental efficiencies. Below certain chargino-neutralino mass differences (3 GeV), the analysis used here becomes completely inoperative. Special low-degeneracy analyses [19] have to be used in order to restore these exclusion areas. Further, a Higgs analysis including MSSM parameter phases, of the type performed in ref. [18], helps to exclude these remaining points, in good complementarity to direct chargino searches.

# 5 The EDM constraints

Further constraints may be obtained from the measurements of the electric dipole moments of the electron and neutron [2, 3]. They are, however, not model independent and require more detailed discussion.

We take into account bounds on the MSSM parameter phases given only by the electron EDM measurement. This is for two reasons. First, the electron EDM depends exactly on the same set of parameters as the cross sections for the chargino and neutralino production, so we do not need to introduce any additional variables in our scan. Second, the theoretical calculation of the neutron EDM is prone to significant QCD uncertainties (see e.g. discussion in [9]), so the limits obtained from its measurements are less established that those given by the electron EDM.

The limits on $\phi_\mu$ coming from the electron EDM measurements also cannot be treated as absolute. In a good approximation, the formulae for the electron EDM can be written down as:

$$d_e \approx d_1 \mathrm{Im}(\mu M_1) \tan\beta + d_2 \mathrm{Im}(\mu M_2) \tan\beta + d_3 \mathrm{Im}(A_e M_1^\star) \tag{25}$$

where coefficients $d_1, d_2, d_3$ depend only on the absolute values of $|M_1|, |M_2|, |\mu|$ and the slepton and sneutrino masses. If $M_1$ and $M_2$ are GUT-related and thus can be both chosen to be real, eq. (25) reduces to:

$$d_e \approx d_\mu \mathrm{Im}(\mu) \tan\beta + d_A \mathrm{Im}(A_e) \tag{26}$$

where for the typical choices of the mass parameters (like the ones we used in our scan) $|d_\mu|/|d_A| \sim \mathcal{O}(10)$, so that $d_e$ is significantly more sensitive to $\phi_\mu$ than to $\phi_{A_e}$, particularly for large $\tan\beta$.

The left-right selectron mixing parameter $A_e$ enters formally the expression for the neutralino production cross section, but it is multiplied there by the electron mass and can be neglected unless $A_e$ is really huge, $|A_e|/m_{\tilde{e}} > \mathcal{O}(10^5)$. Such large values, although not excluded by any experimental measurement, are highly unlikely for theoretical purposes. Therefore, production cross sections of the charginos and neutralinos depend effectively only on the $\mu$ parameter phase, whereas the electron EDM depends on both $\phi_\mu$ and $\phi_{A_e}$. This leaves a possibility of cancellation between phases: for any value of $\mathrm{Im}(\mu)$ one can find a matching value of $\mathrm{Im}A_e$ such that both terms in eq. (26) are almost equal and opposite in sign, so that the electron EDM value predicted by MSSM is below the current experimental bounds. However, as mentioned already in the introduction, such cancellations seems to be entirely accidental (from the point of view of the electroweak scale physics at least) and require strong fine tuning between phases and mass parameters - for light supersymmetric spectrum their values must be correlated with accuracy $\mathcal{O}(10^{-2})$ [9]. Nevertheless, their presence implies that in order to put bounds on the allowed values of $\phi_\mu$ one needs to apply further assumptions.

First, one may naturally assume that the strong fine-tuning between the MSSM parameters required for the cancellations in the electron EDM does not occur. In this case, "generic"

limits on the $\mu$ phase may be obtained assuming that one can neglect the $\mathrm{Im}(A_e)$ term in the $d_e$ expression, setting it to $\mathrm{Im}(A_e) = 0$. We computed the electron EDM values for the points not excluded by the chargino searches analysis and plotted them in figure 15. As can

[width=0.5]edm.eps

Figure 15: Values of the electron EDM calculated for each of the unexcluded points in $(M_2, |\mu|)$ plane, assuming $A_e = 0$, normalized to (divided by) the experimental bound.

be seen from fig. 15, all points are excluded by the condition $|d_e|/d_e^{exp} \leq 1$. Thus, assuming no cancellations between the phases in the electron EDM, the excluded area of the $(M_2, |\mu|)$ plane is not smaller than the one obtained for real negative $\mu$.

Second, one may decide to take into account the possibility of cancellations between the phases in the electron EDM. Then, for most of the mass parameter choices, the relative amplitude of the coefficients $d_\mu$ and $d_A$ in eq. (26) implies that substantial $\mu$ phase requires also large value of the imaginary part of the $A_e$ parameter, $\mathrm{Im}(A_e) \sim \mathcal{O}(10) \times \tan\beta \times \mathrm{Im}(\mu)$, to keep the full electron EDM below the experimental bound. In figure 16 we plot, calculated for each of the unexcluded points on $(M_2, |\mu|)$ plane, the minimal $|\mathrm{Im}(A_e)|$ values required to make $\phi_\mu - \phi_{A_e}$ cancellation in the electron EDM possible. As can be seen from the figure, they depend on the right selectron mass, the larger it is the higher $A_e$ are required[5].

The maximal value of $A_e$ parameter could be constrained if one assumes unification of all LR mixing parameters (both in slepton and squark sectors) at the GUT scale. In such a case, LR mixing parameter in the stop sector should not be larger than $|A_t|/m_{\tilde{t}} \sim \sqrt{3}$, in order to avoid color symmetry breaking [17] and, on the base of the unification assumption, a similar limit may be applied to $A_e$. As can be seen from figure 16, even if we allow for $\phi_\mu - \phi_A$ cancellations, a cut on $|\mathrm{Im}A_e|/m_{\tilde{e}} < 2-3$ eliminates a large fraction of the unexcluded points

[width=0.5]amin.eps

Figure 16: Minimal values of $|\mathrm{Im}A_e|/m_{\tilde{e}}$ necessary for phase cancellation in the electron EDM, calculated for each of the unexcluded points in $(M_2, |\mu|)$ plane, for two choices of the right selectron mass.

on $(M_2, |\mu|)$ plane for right selectron mass of the order of 100 GeV, just above the current experimental bound, and this fraction grows quickly with $m_{\tilde{e}_R}$.

Finally, we comment on the possibility of a non-vanishing phase of the $M_1$ parameter. Such a phase, even if not explicitly present in the chargino mass matrix and expressions for

[5]The "peak structure" visible in the plot is artificial and depends on density of scan over MSSM parameters.

the production cross section, affects the interpretation of chargino searches, through its influence on the decay rates to neutralinos, and through the increased freedom for cancellations in the electron EDM, as obvious from the form of eq. (25) (however, as shown in [9], for light SUSY spectrum such cancellation again require precise fine-tuning between parameter values). Varying $M_1$ phase one changes the physical masses of neutralinos and thus the size of mass splitting between the lightest neutralino and chargino, affecting the experimental efficiency of searches. Hence, the possible impact of the additional phase could be very important. However, from the theoretical point of view, allowing for different phases of $M_1$ and $M_2$ makes sense most likely only if one rejects the assumption of gaugino mass unification, i.e. simultaneously gives up the relation connecting absolute values of masses, $|M_1| = \frac{5}{3}\tan\theta_W^2|M_2|$. In this case $|M_1|$ becomes an additional free parameter and scanning over it one can always find values for which lightest neutralino-chargino mass splitting tends to vanish, so that "standard" chargino searches cannot discover it. Special experimental strategies concerning this experimental "blind spot" have been developed, as mentioned above [19]. These searches, being based on the detection of the SUSY particles through the extra radiation of an initial state photon [20], need the full LEP2 luminosity to become as sensitive as the standard ones, and they will eventually reach close to the kinematical limits only after the end of LEP. Therefore, any meaningful analysis not assuming GUT unification of gaugino masses, i.e. free complex $M_1$ parameter, must take into account these searches, has to await for the end of LEP and is beyond the scope of this paper.

# 6 Conclusions

In conclusion, we recalculated the production and decay rates of charginos and neutralinos at LEP, in the case of complex MSSM parameters. We performed an extensive scan over the relevant MSSM parameters and compared the expected signals to data from DELPHI, taken at 189 GeV. We extend the standard LEP analyses by scanning also over the $\mu$ phase. This is the only new phase to which these processes are sensitive, if one assumes $M_1, M_2$ unification at the GUT scale. The inclusion of $\mu$ phase introduces new points of degeneracy between the chargino and neutralino masses, lowering the chargino detection efficiency. It can also lead to cross-sections lower than the ones obtained for real $\mu$ values and mildly affects the decay branching ratios. We found that the limits obtained by the experimental collaboration, which do not take into account the non-trivial $\mu$ phase are in general robust, apart from the case of low $\tan\beta$ and low sneutrino mass for which unexcluded points appear in a region around $M_2 \sim \tan\beta|\mu|$. These points can be excluded, restoring the real-case limits, if one takes into account the limits on new physics obtained by the measurement of the $Z^0$ width and

the experimental constraints on electron EDM. The latter statement assumes that $\mathrm{Im}(A_e)$ is not precisely fine-tuned so that it cancels the $\mathrm{Im}(\mu)$ contribution to the EDM. Apart, possibly, from cases of extreme degeneracy between charginos and neutralinos induced by phases, present anyway also in the real-parameter case, we found no fundamental loophole in the LEP exclusions that would not be covered by the final LEP luminosity. Further, the influence of $\mu$ phase is more prominent for low $\tan\beta$, in a region where Higgs negative searches can give complementary exclusions, provided they are also made under the assumption of complex MSSM parameters.


## Acknowledgments

We would like to acknowledge discussions with J.F. Grivaz, G. Kane, F. Richard, S. Pokorski, M. Winter and many members of the "CNRS, Groupement De Recherche sur la Supersymétrie" as well as the extremely valuable help of T. Alderweireld and P. Rebecchi who provided us with the DELPHI data.


# Appendix Conventions and Feynman rules

For easy comparison with other references we spell out our conventions. They are similar to the ones used in ref. [12]. We present only the part of the MSSM Lagrangian which we are interested in, i.e. electroweak interactions of gauge, Higgs and slepton supermultiplets. The MSSM matter fields form chiral left-handed superfields in the following representations of the $SU(2) \times U(1)$ gauge group (the generation index is suppressed):

| Scalar field | Weyl Fermion field | $SU(2) \times U(1)$ representation |
|---|---|---|
| $L = \begin{pmatrix} \tilde{\nu}_0 \\ E \end{pmatrix}$ | $l = \begin{pmatrix} \nu \\ e \end{pmatrix}$ | $(2,-1)$ |
| $E^c$ | $e^c$ | $(0,2)$ |
| $H^1 \begin{pmatrix} H_1^1 \\ H_2^1 \end{pmatrix}$ | $\tilde{h}^1 \begin{pmatrix} \tilde{h}_1^1 \\ \tilde{h}_2^1 \end{pmatrix}$ | $(2,-1)$ |
| $H^2 \begin{pmatrix} H_1^2 \\ H_2^2 \end{pmatrix}$ | $\tilde{h}^2 \begin{pmatrix} \tilde{h}_1^2 \\ \tilde{h}_2^2 \end{pmatrix}$ | $(2,1)$ |

Two $SU(2)$-doublets can be contracted into an $SU(2)$-singlet, e.g. $H^1H^2 = \epsilon_{ij}H_i^1H_j^2 = -H_1^1H_2^2 + H_2^1H_1^2$ (we choose $\epsilon_{12} = -1$; lower indices (when present) will label components of $SU(2)$-doublets). The superpotential and the soft terms are defined as:

$$W = Y_e H^1 L E + \mu H^1 H^2 \tag{A.1}$$

$$\begin{aligned}\mathcal{L}_{soft} &= -M_{H^1}^2 H^{1\dagger} H^1 - M_{H^2}^2 H^{2\dagger} H^2 - L^\dagger M_L^2 L - E^{c\dagger} M_E^2 E^c \\ &+ \left(\frac{1}{2} M_2 \tilde{W}^i \tilde{W}^i + \frac{1}{2} M_1 \tilde{B}\tilde{B} + m_{12}^2 H^1 H^2 + Y_e A_e H^1 L E^c + \text{H.c.}\right) \end{aligned} \tag{A.2}$$

where we extracted Yukawa coupling matrices from the definition of the $A_e$ coefficient.

In general, the Yukawa couplings and the masses are matrices in the flavor space. Simultaneous rotation of the fermion and sfermion fields can diagonalize the Yukawa couplings (and simultaneously fermion mass matrices), leading to so-called "super-KM" basis, with flavor diagonal Yukawa couplings and neutral current fermion and sfermion vertices. We give all the expressions already in the super-KM basis (see e.g. [11] for a more detailed discussion).

The slepton mass matrices in the super-KM basis have the following form:

$$\begin{aligned}\mathcal{M}_{\tilde{L}}^2 &= \begin{pmatrix} M_L^2 + m_e^2 + \frac{\cos 2\beta}{2}(M_Z^2 - 2M_W^2)\hat{1} & -m_e(\tan\beta\mu\hat{1} + A_e^\star) \\ -m_e(\tan\beta\mu^\star\hat{1} + A_e) & M_E^2 + m_e^2 - \cos 2\beta(M_Z^2 - M_W^2)\hat{1} \end{pmatrix} \\ \mathcal{M}_{\tilde{\nu}}^2 &= M_L^2 + \frac{\cos 2\beta}{2} M_Z^2 \hat{1} \end{aligned} \tag{A.3}$$

where $\theta_W$ is the Weinberg angle and $\hat{1}$ stands for the $3 \times 3$ unit matrix.

The matrices $\mathcal{M}_{\tilde{\nu}}^2$ and $\mathcal{M}_{\tilde{L}}^2$ can be diagonalized by additional unitary matrices $Z_\nu$ $(3 \times 3)$ and $Z_L$ $(6 \times 6)$, respectively

$$\left(\mathcal{M}_{\tilde{\nu}}^2\right)^{diag} = Z_\nu^\dagger \mathcal{M}_{\tilde{\nu}}^2 Z_\nu \qquad\qquad \left(\mathcal{M}_{\tilde{L}}^2\right)^{diag} = Z_L^\dagger \mathcal{M}_{\tilde{L}}^2 Z_L \tag{A.4}$$

The physical (mass eigenstates) sleptons are then defined in terms of super-KM basis fields (A.1) as:

$$\tilde{\nu} = Z_\nu^\dagger \tilde{\nu}_0 \qquad\qquad \tilde{L} = Z_L^\dagger \begin{pmatrix} E \\ E^{c\star} \end{pmatrix} \tag{A.5}$$

Throughout this paper we assume that the flavor and CP violation due to the flavor mixing in the sfermion mass matrices is negligible from the point of view of chargino and neutralino production, i.e. matrices $M_{L,E}^2, A_e$ are almost diagonal in the super-KM basis, so that also $Z_{\tilde{\nu}}, Z_L \approx \hat{1}$. However, one should remember that even such very small values of the $A_e$ parameter, if contain imaginary part, may affect bounds on the $\mu$ phase given by the EDM measurements.

The physical Dirac chargino and Majorana neutralino eigenstates are linear combinations of left-handed Winos, Binos and Higgsinos

$$\chi_i^+ = \begin{pmatrix} -iZ_+^{i1\star}\tilde{W^+} + Z_+^{i2\star}\tilde{h}_2^1 \\ iZ_-^{i1}\overline{\tilde{W^-}} + Z_-^{i2}\overline{\tilde{h}_1^2} \end{pmatrix} \tag{A.6}$$

where $\tilde{W}^{\pm} = (\tilde{W}^1 \mp \tilde{W}^2)/\sqrt{2}$.

$$\chi_i^0 = \begin{pmatrix} -iZ_N^{i1\star}\tilde{B} - iZ_N^{i2\star}\tilde{W}^3 + Z_N^{i3\star}\tilde{h}_1^1 + Z_N^{i4\star}\tilde{h}_2^2 \\ iZ_N^{i1}\overline{\tilde{B}} + iZ_N^{i2}\overline{\tilde{W}^3} + Z_N^{i3}\overline{\tilde{h}_1^1} + Z_N^{i4}\overline{\tilde{h}_2^2} \end{pmatrix} \tag{A.7}$$

The unitary transformations $Z^+$, $Z^-$ and $Z_N$ diagonalize the mass matrices of these fields

$$\mathcal{M}_C = Z_-^T \begin{pmatrix} M_2 & \frac{gv_2}{\sqrt{2}} \\ \frac{gv_1}{\sqrt{2}} & \mu \end{pmatrix} Z_+ \tag{A.8}$$

and

$$\mathcal{M}_N = Z_N^T \begin{pmatrix} M_1 & 0 & -\frac{g'v_1}{2} & \frac{g'v_2}{2} \\ 0 & M_2 & \frac{gv_1}{2} & -\frac{gv_2}{2} \\ -\frac{g'v_1}{2} & \frac{gv_1}{2} & 0 & -\mu \\ \frac{g'v_2}{2} & -\frac{gv_2}{2} & -\mu & 0 \end{pmatrix} Z_N \tag{A.9}$$

Using the notation of this Appendix, one can list (in the mass eigenstate basis) the Feynman rules necessary to calculate cross sections (3),(11) and (20),(21):

1) Interactions of charginos and sneutrinos:

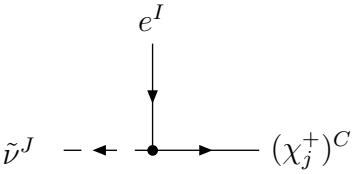


$$i\left(S_{LC}^{IJi}P_L + S_{RC}^{IJi}P_R\right)$$

where

$$S_{LC}^{IJi} = -g_2 Z_{1j}^+ Z_{\tilde{\nu}}^{IJ\star} \tag{A.10}$$

$$S_{RC}^{IJi} = \frac{m_e^I\sqrt{2}}{v_1} Z_{2j}^{-*} Z_{\tilde{\nu}}^{IJ\star} \tag{A.11}$$

2) Interactions of charginos and neutralinos with gauge bosons:

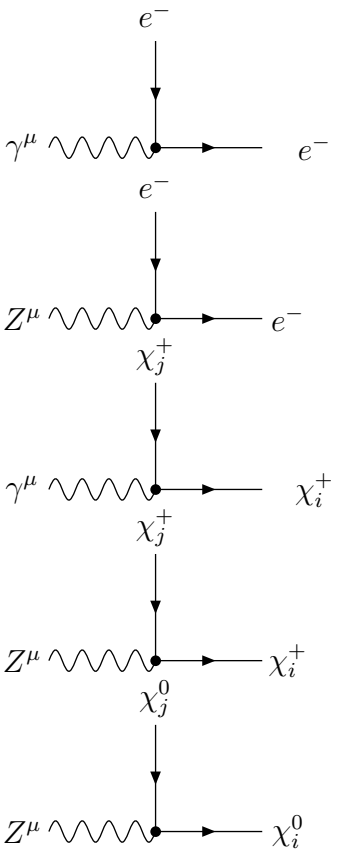


$-ie\gamma^\mu$

$ie\gamma^\mu(a_e P_L + b_e P_R)$

$ie\gamma^\mu\delta_{ij}$

$i\gamma^\mu\left(V_{LC}^{ij}P_L + V_{RC}^{ij}P_R\right)$

$i\gamma^\mu\left(V_N^{ij}P_L - V_N^{ij\star}P_R\right)$

where

$$V_{LC}^{ij} = -\frac{e}{2\sin\theta_W\cos\theta_W}(Z_{1i}^{+*}Z_{1j}^{+} + \delta^{ij}\cos 2\theta_W) \quad (A.12)$$

$$V_{RC}^{ij} = -\frac{e}{2\sin\theta_W\cos\theta_W}(Z_{1i}^{-}Z_{1j}^{-*} + \delta^{ij}\cos 2\theta_W) \quad (A.13)$$

$$V_N^{ij} = \frac{e}{2\sin\theta_W\cos\theta_W}(Z_N^{4i*}Z_N^{4j} - Z_N^{3i*}Z_N^{3j}) \quad (A.14)$$

# References


[1] M. Brhlik and G.L. Kane, *Phys. Lett.* **B437**, (1998) 331, A. Pilaftsis, C.E.M. Wagner, *Nucl. Phys.* **B553** (1999) 3-42; M. Carena, J. Ellis, A. Pilaftsis, C.E.M. Wagner, *Nucl. Phys.* **B586** (2000) 92-140.

[2] E. Commins *et al.*, *Phys. Rev.* **A50** (1994) 2960; K. Abdullah *et al.*, *Phys. Rev. Lett.* **65** (1990) 234.

[3] P. G. Harris *et al.*, *Phys. Rev. Lett.* **82**, (1999) 904.

[4] J. Ellis, S. Ferrara and D.V. Nanopoulos, *Phys. Lett.* **114B** (1982) 231; W. Buchmüller and D. Wyler, *Phys. Lett.* **121B** (1983) 321; J. Polchinski and M.B. Wise *Phys. Lett.*

**125B** (1983) 393; J.M. Gerard *et al.*, *Nucl. Phys.* **B253** (1985) 93; P. Nath, *Phys. Rev. Lett.* **66** (1991) 2565; Y. Kizuruki and N. Oshimo. *Phys. Rev.* **D45** (1992) 1806; *Phys. Rev.* **D46** (1992) 3025; R. Garisto, *Nucl. Phys.* **B419** (1994) 279.

[5] T. Falk, K.A. Olive *Phys. Lett.* **B439** (1998) 71; *Phys. Lett.* **B375** (1996) 196.

[6] T. Ibrahim and P. Nath, *Phys. Lett.* **B418** (1998) 98; *Phys. Rev.* **D57** (1998) 478; *Phys. Rev.* **D58** (1998) 111301.

[7] A. Bartl, T. Gajdosik, W. Porod, P. Stockinger and H. Stremnitzer, *Phys. Rev.* **D60** (1999) 073003.

[8] M. Brhlik, G.J. Good and G.L. Kane, *Phys. Rev.* **D59** (1999) 115004.

[9] S. Pokorski, J. Rosiek and C. Savoy, *Nucl. Phys.* **B570** (2000) 81-116.

[10] M. Brhlik, L. Everett, G.L. Kane, J. Lykken, *Phys. Rev. Lett.* **83** (1999) 2124-2127.

[11] M. Misiak, J. Rosiek, S. Pokorski, *hep-ph*/9703442, published in A. Buras, M. Lindner (eds.), *Heavy flavours II*, pp. 795-828, World Scientific Publishing Co., Singapore.

[12] J. Rosiek, *Phys. Rev.* **D41**, (1990) 3464, *erratum hep-ph*/9511250.

[13] N. Ghodbane *et. al.*, *hep-ph*/9909499.

[14] S. Y. Choi, M. Guchait, J. Kalinowski, P. M. Zerwas, *Phys. Lett.* **B479** (2000) 235-245; S. Y. Choi, A. Djouadi, M. Guchait, J. Kalinowski, H. S. Song, P. M. Zerwas, *Eur. Phys. J.* **C14** (2000) 535-546.

[15] *Search for charginos in* $e^+e^-$ *interactions at* $\sqrt{s} = 189$ *GeV.* DELPHI collaboration *CERN-EP 2000-008*, accepted for publication at Physics Letters.

[16] K. Mönig, *Model independent limit of the Z-decays Width into Unknown particles*, DELPHI 97-174 PHYS 748.

[17] J.A. Casas, A. Lleyda, C. Munoz, *Nucl. Phys.* **B471** (1996) 3-58.

[18] G. L. Kane, L. Wang, *Phys. Lett.* **B488** (2000) 383-389.

[19] DELPHI Collaboration "Search for charginos nearly mass-degenerate with the lightest neutralino", *Eur. Phys. J.* **C11** (1999) 1; L3 Collaboration, *Phys. Lett.* **B482** (2000) 31.

[20] C-H. Chen, M. Drees, J.F. Gunion, *Phys. Rev.* **D55** (1997) 330-347; *erratum ibid* **D60** (1999) 039901.